A DFT Study on the Mechanism of Cyclopropanation via $Cu(acac)_2$-Catalyzed Diazo Ester Decomposition

Cihan Özen and Nurcan Ş. Tüzün*

Department of Chemistry, Faculty of Science and Letters, Istanbul Technical University, 34469 Maslak, Istanbul, Turkey

Received February 1, 2008

The mechanism of the copper(I)-catalyzed olefin cyclopropanation reaction with dimethyl diazomalonate has been extensively investigated using the DFT method at B3LYP/6-31G* and BP86/SDD/6-31G* levels. All the possible pathways leading first to a metal carbene and then to the cyclopropane product have been studied with ethene as a model substrate and their energetics are demonstrated. Then the suggested mechanisms were applied to a real system: namely, 2,2-dimethyl-4,7-dihydro-1,3-dioxepine.

Introduction

Cyclopropane derivatives are attractive to organic chemists, since they occur very frequently as starting compounds or subunits in biologically active natural and synthetic products.[1,2] One of the most common methods of synthesizing cyclopropanes is transition-metal-catalyzed decomposition of diazo esters with olefins.[1,3] Several cyclopropane systems obtained via transition-metal-catalyzed systems with high diastereo- and enantioselectivities have been reported in the literature.[4] In this transformation, metal-complexed carbenes are produced which are the key intermediates that further react to form the final cyclopropane product. A great deal of research has concentrated on the use of copper complexes[5] because of their cheapness and efficiency.[6] Historically, Nozaki et al. accomplished the first enantioselective cyclopropanation reaction using copper salicylaldimine.[7] Then Aratani's asymmetric process of cyclopropanation via Cu-based catalysts following Nozaki's work brought metal-mediated transformation of alkene to large-scale industrial production.[8] In experimental studies, the copper carbene complexes are rarely observed by spectroscopic methods, due to the high reactivity of copper catalysts for diazo ester decomposition.[9] Only two copper complexes have been detected by ultra-low-temperature NMR.[10] Other transition-metal carbene species, such as those of ruthenium and osmium, have been isolated from stoichiometric reactions with diazo esters.[11]

Although there have been experimental studies on cyclopropanation via copper-catalyzed diazo decomposition, the theoretical work on copper carbene formation is rather scarce. In mechanistic studies on copper-catalyzed cyclopropanation reactions, some points are agreed upon by all studies. First, the entire mechanism consists of two parts. These are the copper carbene formation and the cyclopropanation stages (Figure 1).

It was formerly thought that both Cu(I) and Cu(II) were active catalytic species; however, the kinetic data by Kochi et al. have shown Cu(I) to be a more active species than Cu(II). Cu(II) is reduced to Cu(I) by diazo compounds.[12] Nowadays, generally, Cu(I) is prepared in situ, but little information is known about how it forms the carbene structure.[3]

Thermodynamically, the N_2 extrusion step has been stated to have the highest overall Gibbs free energy in diazo ester decomposition reactions. Therefore, in the literature, this step is considered as the rate-determining step.[12−14] There are mainly two possibilities for copper carbene formation via N_2 extrusion: olefin assisted and olefin nonassisted.[13] In the nonassisted mechanism[13−15] olefin is detached from catalyst before N_2 extrusion, whereas in the assisted mechanism,[16] the olefin molecule is bonded to the catalyst until the metal carbene forms.

At the cyclopropanation stage, the reaction can be completed by going through either a three-centered or a four-

(1) Doyle, M. P.; McKervey, A.; Ye, T. *Modern Catalytic Methods for Organic Synthesis with Diazo Compounds*; Wiley: New York, 1998; Chapters 2 and 4.

(2) (a) Suckling, C. J. *Angew. Chem., Int. Ed. Engl.* **1988**, *27*, 537–552. (b) Wong, H. N. C.; Hon, M.-Y.; Tse, C.-W.; Yip, Y.-C.; Tanko, J.; Hudlicky, T. *Chem. Rev.* **1989**, *89*, 165–198.

(3) Kirmse, W. *Angew. Chem., Int. Ed.* **2003**, *42*, 1088–1093.

(4) (a) Rasmussen, T.; Jensen, J. F.; Østergaard, N.; Tanner, D.; Ziegler, T.; Norrby, P. *Chem. Eur. J.* **2002**, *8*, 177–184. (b) Lo, M. M.-C.; Fu, G. C. *J. Am. Chem. Soc.* **1998**, *120*, 10270–10271. (c) Cavallo, L.; Cucciolito, M. E.; De Martino, A.; Giordano, F.; Orabona, I.; Vitagliano, A. *Chem. Eur. J.* **2000**, *6* (7), 1127–1139. (d) Wilson, P. D.; Lyle, M. P. A. *Org. Lett,* **2004**, *6* (5), 855–857. (e) Doyle, M. P.; Davies, S. B.; Hu, W. *Org. Lett.* **2000**, *2* (8), 1145–1147.

(5) (a) Díaz-Requejo, M. M.; Pérez, P. *J. Organomet. Chem.* **2000**, *690*, 5441–5450. (b) Padwa, A.; Austin, D. J. *Angew. Chem., Int. Ed.* **1994**, *33*, 1797–1815.

(6) Pfaltz, A. Cyclopropanation and C-H Insertion with Cu. In *Comprehensive Asymmetric Catalysis*; Jacobsen, E. N., Pfaltz, A., Yamamoto, H., Eds.; Springer-Verlag: Berlin, 1999; Vol. 2, pp 513−538.

(7) Nozaki, H.; Moriuti, S.; Takaya, H.; Noyori, R. *Tetrahedron Lett.* **1966**, 5239–5244.

(8) Aratani, T. *Pure Appl. Chem.* **1985**, *57*, 1839–1844.

(9) Pfaltz A. In *Comprehensive Asymmetric Catalysis*; Jacobsen, E. N., Pfaltz, A., Yamamoto, H., Eds.; Springer: Berlin, 1999; Vol. I−III, Chapter 16.1, p 3.

(10) Straub, B. F.; Hofmann, P. *Angew. Chem. Int. Ed* **2001**, *40* (7), 1288–1290.

(11) (a) Smith, D. A.; Reynolds, D.; Woo, L. *J. Am. Chem. Soc.* **1993**, *155*, 2511–2513. (b) Park, S. B.; Sokata, N.; Nishiyama, H. *Chem. Eur. J.* **1996**, *2*, 303–306.

(12) Salomon, R. G.; Kochi, J. K. *J. Am. Chem. Soc.* **1973**, *95*, 3300–3310.

(13) Fraile, J. M.; García, J. I.; Martinez-Merino, V.; Mayoral, J. A.; Salvatella, L. *J. Am. Chem. Soc.* **2001**, *123*, 7616–7625.

(14) Straub, B. F.; Gruber, I.; Rominger, F.; Hofmann, P. J. *J. Organomet. Chem.* **2003**, *684*, 124–143.

(15) Meng, Q.; Tang, D.; Shen, W.; Zhang, J. *J. Mol. Struct. (THEOCHEM)* **2004**, *711*, 193–199.

(16) Bühl, M.; Terstegen, F.; Löffler, F.; Meynhardt, B.; Kierse, S.; Müller, M.; Näther, C.; Lüning, U. *Eur. J. Org. Chem.* **2001**, 2151–2160.

10.1021/om800094k CCC: $40.75
Publication on Web 08/22/2008

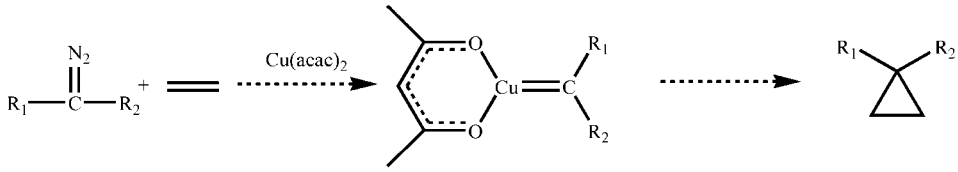

Figure 1. Stages of the cyclopropanation reaction (R_1 = $COOCH_3$, R_2 = H, $COOCH_3$).

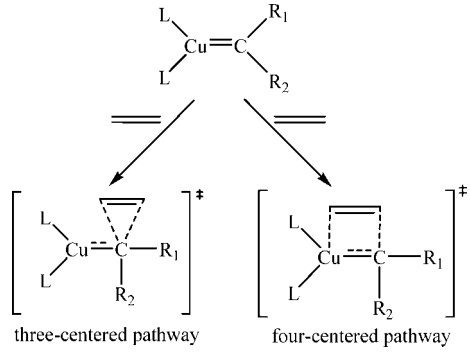

Figure 2. Possible cyclopropanation mechanism.

centered activated complex (Figure 2). In the three-centered pathway, olefin directly adds to the carbene carbon, whereas in the four-centered complex, a metallacyclobutane intermediate is formed initially.

In this study, copper carbene complex formation and cyclopropanation reactions have been studied by starting with ethene as the substrate, dimethyl diazomalonate (DMDM) as the diazo compound, and copper(II) acetylacetonate [$Cu(acac)_2$] as the transition-metal catalyst in light of the aforementioned literature findings. First, a model compound, ethene, and then a real substrate, 2,2-dimethyl-4,7-dihydro-1,3-dioxepine, which is reported to produce a cyclopropane product,[17] will be modeled through possible mechanisms by quantum-mechanical calculations. This work aims to shed light on the underlying catalytic reaction mechanism in full detail, since better mechanistic insight should help in the development of better catalysts or in obtaining tailor-made products.

Methodology

In the context of this study, all the possible reaction mechanisms, including intermediates and transition states, have been modeled and discussed in terms of relative energies obtained from quantum-mechanical calculations. The DFT method employing the B3LYP functional[18] with the 6-31G* basis set has been used to carry out the full optimization of the compounds of interest in the gas phase with the G03 package.[19] The DFT methodology with B3LYP functional has been shown to give reliable results in transition metals, including copper-catalyzed cyclopropanations.[13,20,21] BP86/SDD/6-31G* calculations have also been performed on the structures discussed in this study to see the effect of a different methodology on the mechanism. In the literature, the BP86 functional[22] at the 6-31G* basis set for C, N, O, and H atoms and the SDD effective-core potential[23] for Cu have been stated to give reliable results.[24] Throughout the discussion that follows, energetics from B3LYP/6-31G* calculations will be referred to unless otherwise stated and the BP86/SDD/6-31G* energies will be given in parentheses where available.

The stationary points were analyzed by vibrational frequency calculations. All transition states were verified to be saddle points by one imaginary frequency belonging to the reaction coordinate. IRC[25] calculations have been performed on transition states to obtain minima on both sides. The energies discussed in the text are Gibbs free energies calculated at 298 K, unless otherwise stated.

NBO[26] analysis has been carried out on some structures in order to investigate the stabilizing donor−acceptor interactions and the nature of the Cu−C bonds in some selected structures.

Three-dimensional structures are from the B3LYP/6-31G* calculations unless otherwise stated, and those not included in the text are presented in the Supporting Information. In some of the figures, critical bond lengths are shown (in Å) and hydrogens have been omitted for clarity. In general, cyclopropanation reactions via carbenes are performed in nonpolar solvents such as dichloromethane; thus, significant solvent effects are not expected in these reactions. The effect of solvent was considered for the reactions in Schemes 1−3 by single-point SCRF calculations with the IEF-PCM[27] method at the B3LYP/6-31G* level. The free energies in dichloromethane were

(17) Talınlı, N.; Karliğa, B.; Anaç, O. *Helv. Chim. Acta* **2000**, *83*, 966–971.

(18) (a) Becke, A. D. *J. Chem. Phys.* **1993**, *98*, 5648–5652. (b) Lee, C.; Yang, W.; Parr, R. G. *Phys. Rev B.* **1988**, *37*, 785–789.

(19) Frisch, M. J.; Trucks, G. W.; Schlegel, H. B.; Scuseria, G. E.; Robb, M. A.; Cheeseman, J. R.; Montgomery, J. A.; Vreven, T., Jr.; Kudin, K. N.; Burant, J. C.; Millam, J. M.; Iyengar, S. S.; Tomasi, J.; Barone, V.; Mennucci, B.; Cossi, M.; Scalmani, G.; Rega, N.; Petersson, G. A.; Nakatsuji, H.; Hada, M.; Ehara, M.; Toyota, K.; Fukuda, R.; Hasegawa, J.; Ishida, M.; Nakajima, T.; Honda, Y.; Kitao, O.; Nakai, H.; Klene, M.; Li, X.; Knox, J. E.; Hratchian, H. P.; Cross, J. B.; Adamo, C.; Jaramillo, Gomperts, R.; Stratmann, R. E.; Yazyev, O.; Austin, A. J.; Cammi, R.; Pomelli, C.; Ochterski, J. W.; Ayala, P. Y.; Morokuma, K.; Voth, G. A.; Salvador, P.; Dannenberg, J. J.; Zakrzewski, V. G.; Dapprich, S.; Daniels, A. D.; Strain, M. C.; Farkas, O.; Malick, D. K.; Rabuck, A. D.; Raghavachari, K.; Foresman, J. B.; Ortiz, J. V.; Cui, Baboul, A. G.; Clifford, S.; Cioslowski, J.; Stefanov, B. B.; Liu, G.; Liashenko, A.; Piskorz, P.; Komaromi, Martin, R. L.; Fox, D. J.; Keith, T.; Al-Laham, M. A.; Peng, C. Y.; Nanayakkara, A.; Challacombe, M.; Gill, P. M. W.; Johnson, B.; Chen, W.; Wong, M. W.; Gonzalez, C.; Pople, J. A. Gaussian 03, Revision C.02; Gaussian, Inc., Wallingford, CT, 2004.

(20) (a) Niu, S.; Hall, M. B. *Chem. Rev.* **2000**, *100*, 353–406. (b) Diedenhofen, M.; Wagener, T.; FrenkingG. In *Computational Organometallic Chemistry*; Cundari, T., Ed.; Marcel Dekker: New York, 2001; pp 69−121. (c) Schultz, N. E.; Zhao, Y.; Truhlar, D. G. *J. Phys. Chem. A* **2005**, *109* (19), 4388–4403. (d) Neese, F. *J. Chem. Phys.* **2003**, *118*, 3939–3948.

(21) Suenobu, K.; Itagaki, M.; Nakamura, E. *J. Am. Chem. Soc.* **2004**, *126*, 7271–7280.

(22) (a) Becke, A. D. *Phys. Rev. A* **1988**, *38*, 3098–3100. (b) Perdew, J. P. *Phys. Rev. B* **1986**, *33*, 8822–8824. (c) Perdew, J. P. *Phys. Rev. B* **1986**, *34*, 7406.

(23) Fuentealba, P.; Preuss, H.; Stoll, H.; von Szentpaly, L. *Chem. Phys. Lett.* **1989**, *89*, 418–422.

(24) Bühl, M.; Kabrede, H. *J. Chem. Theory Comput.* **2006**, *2*, 1282–1290.

(25) (a) Gonzalez, C.; Schlegel, H. B. *J. Phys. Chem.* **1990**, *94*, 5523–5527. (b) Gonzalez, C.; Schlegel, H. B. *J. Chem. Phys.* **1989**, *90*, 2154–2161.

(26) (a) Foster, P.; Weinhold, F. *J. Am. Chem. Soc.* **1980**, *102*, 7211–7218. (b) Reed, A.; Weinhold, E. F. *J. Chem. Phys.* **1983**, *78*, 4066–4073. (c) Reed, A. E.; Weihstock, R. B.; Weinhold, F. *J. Chem. Phys.* **1985**, *83*, 735–746. (d) Reed, A. E.; Weinhold, F. *J. Chem. Phys.* **1985**, *83*, 1736–1740. (e) Reed, A. E.; Curtiss, L. A.; Weinhold, F. *Chem. Rev.* **1988**, *88*, 899–926.

(27) (a) Tomasi, J.; Mennucci, B.; Cancés, E. *J. Mol. Struct. (THEOCHEM)* **1999**, *464*, 211–226. (b) Cossi, M.; Scalmani, G.; Rega, N.; Barone, V. *J. Chem. Phys.* **2002**, *117*, 43–54.

Scheme 1. Olefin-Assisted Copper Carbene Formation from Ethene Complex 3[a]

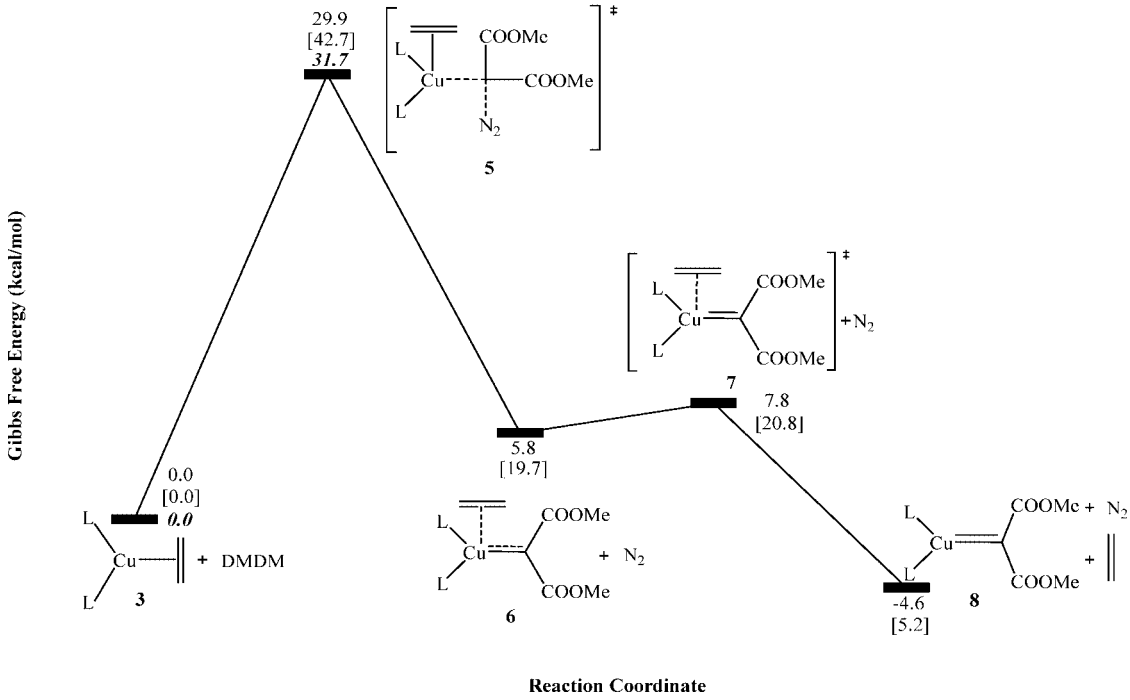

[a] Gibbs free energies refer to B3LYP/6-31G*. Values in parentheses refer to BP86/SDD/6-31G* results with ethene, and bold italic values refer to B3LYP/6-31G* calculations with dioxepine as substrate.

Scheme 2. Olefin Nonassisted Copper Carbene Formation from Ethene Complex 3[a]

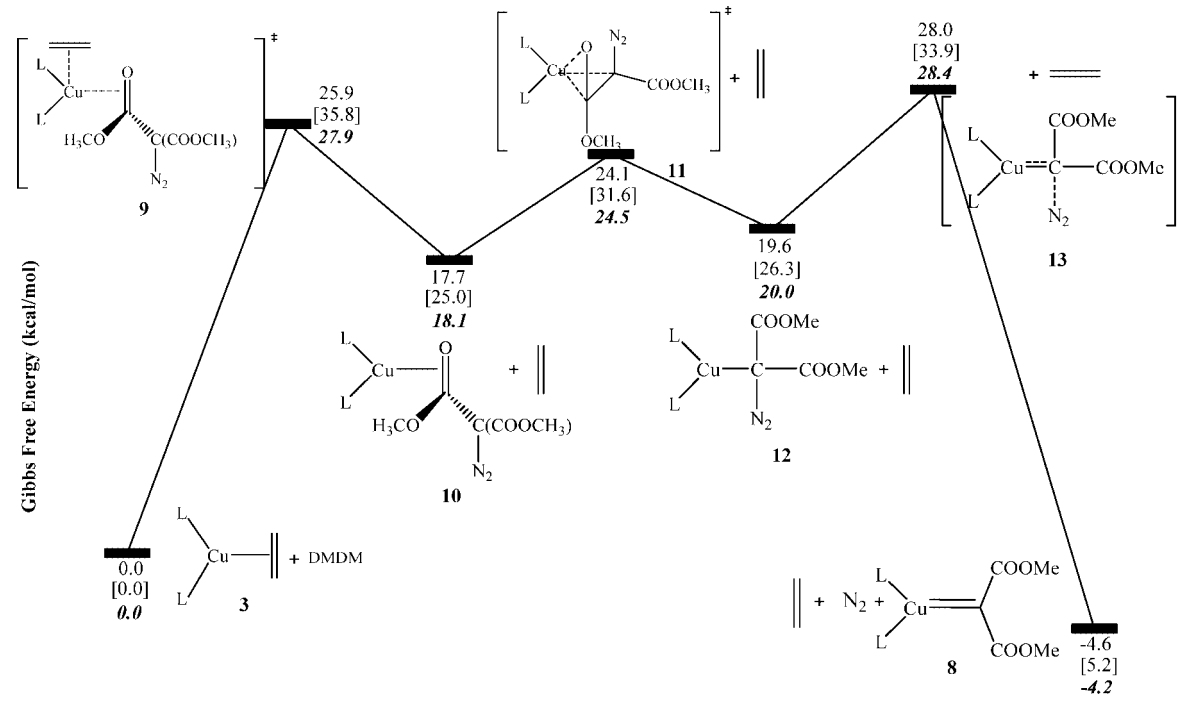

[a] Gibbs free energies refer to B3LYP/6-31G*. Values in parentheses refer to BP86/SDD/6-31G* results with ethene, and bold italic values refer to B3LYP/6-31G* calculations with dioxepine as substrate.

obtained by using the frequencies for the gas-phase results. These calculations, submitted in Schemes S3−S5 in the Supporting Information, have revealed no significant change in trends. Furthermore, two of the most dipolar species considered, structures **20** and **22**, are optimized in solvent with the IEF-PCM[27] method at the B3LYP/6-31G* level. Confirming our expectations, neither geometries nor the relative energies changed significantly as compared to the gas-phase results (Figure S1 in the Supporting Information). These findings are in accordance with the literature, where the uncharged copper complexes were

Scheme 3. Olefin Nonassisted Copper Carbene Formation from Ethene Complex 3[a]

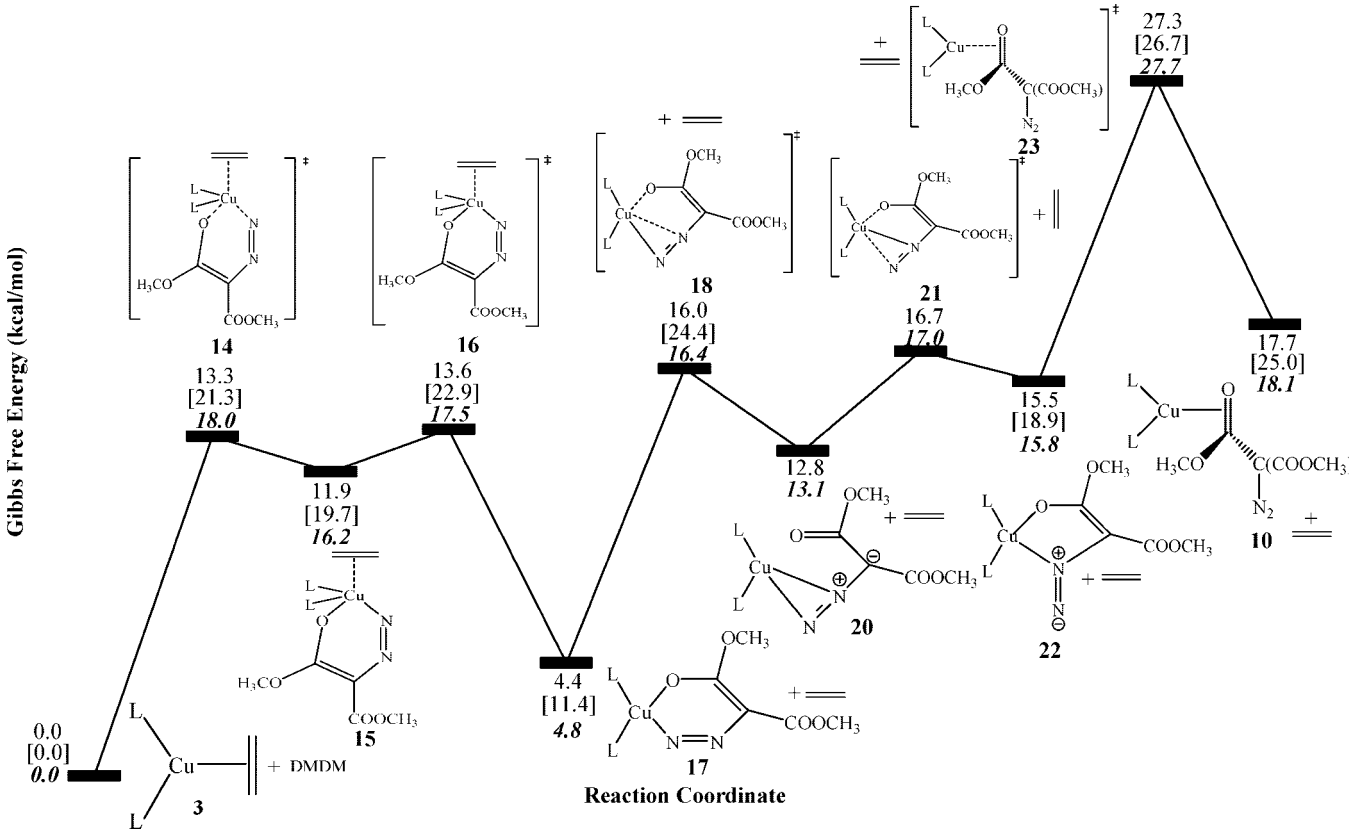

[a] Gibbs free energies refer to B3LYP/6-31G*. Values in parentheses refer to BP86/SDD/6-31G* results with ethene, and bold italic values refer to B3LYP/6-31G* calculations with dioxepine as substrate.

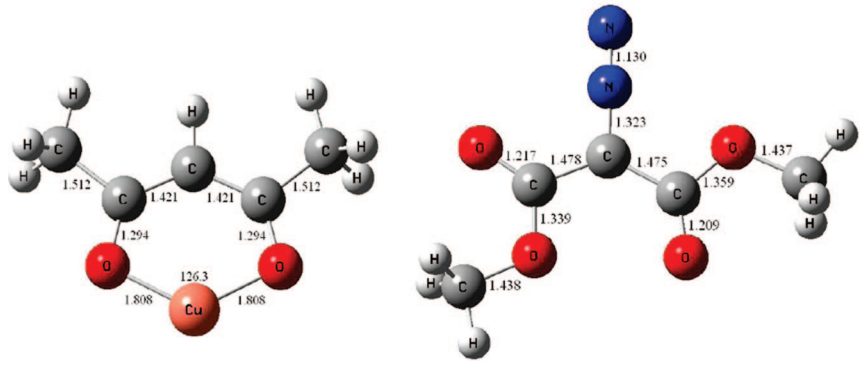

Figure 3. Reduced form of the copper(II) catalyst (**1**) and DMDM (**2**).

reported to minimize solvation artifacts when comparing computed gas -phase energies with experimental chemistry in hydrocarbon solutions.[14,21]

Results and Discussion

The active form of the catalyst, Cuacac (**1**) (Figure 3), and the diazo compound, dimethyl diazomalonate (DMDM), have planar structures due to the extended conjugations they have, as shown in Figure 3. The conformation of DMDM, where the carbonyl groups are syn to each other, is slightly more stable (0.2 kcal/mol) than the anti.

The transformation of catalyst−ethylene species to catalyst−diazo compounds can occur via associative or dissociative displacement. In the dissociative displacement, naked catalyst binds to the diazo compound, whereas in the associative displacement, it is the catalyst−ethylene complex that binds to the diazo compound. In this system, the sum of the energies of components in the dissociative displacement reaction is 38.8 kcal/mol higher in energy than that of the associative path (Figure 4), in accordance with other quantum-mechanical calculations on analogous systems.[15,16] On the other hand, experimenters have proposed the dissociative pathway as favorable,[1,3] which presented conflict between theoretical and experimental work. This discrepancy has been stated to stem from the absence of solvent molecules in calculations[3] and the lack of detailed mechanistic experimental investigation on the mechanism of copper carbene and cyclopropanation reactions.[21]

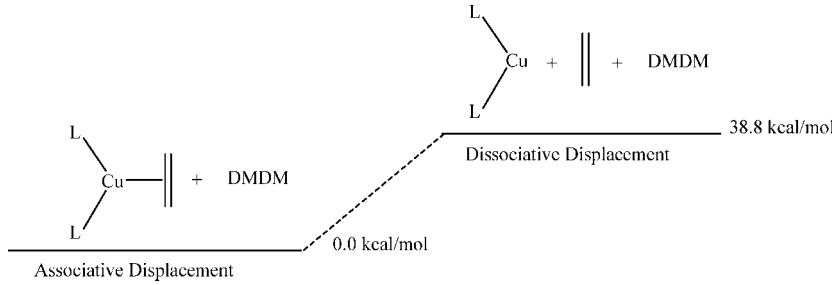

Figure 4. Relative energies of the sum of components in associative and dissociative displacements.

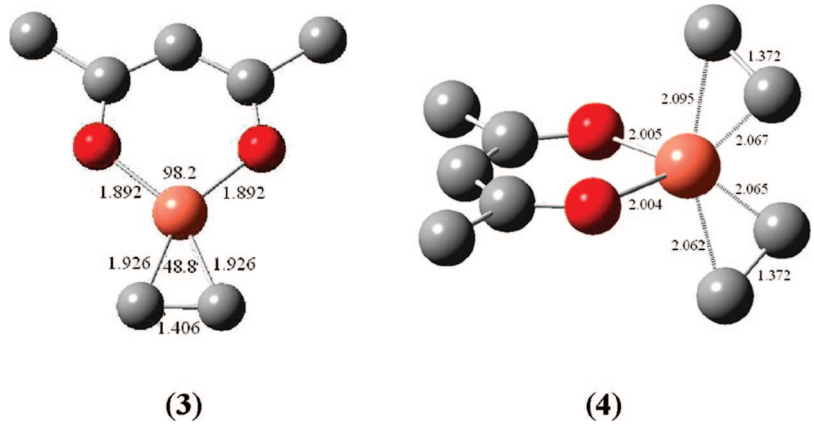

(3) **(4)**

Figure 5. 1:1 and 1:2 catalyst−ethylene complexes.

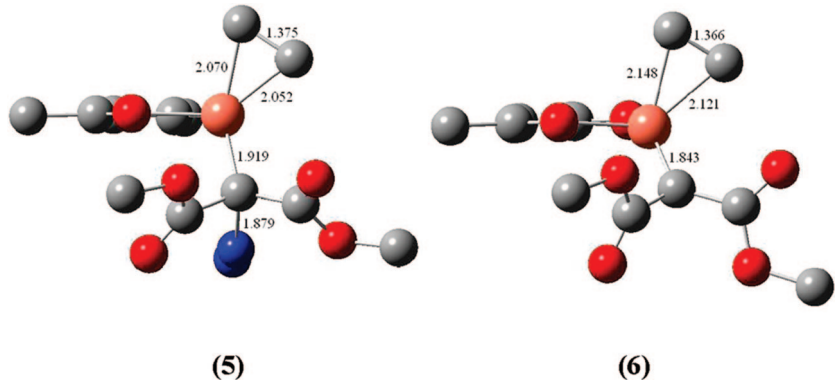

(5) **(6)**

Figure 6. Three-dimensional geometrical structures of **5** and **6**.

According to kinetic studies, excess olefin retards the rate of the cyclopropanation reaction because of the pre-equilibrium[28] involving the catalyst−olefin complexes, where catalyst−olefin stoichiometries of 1:1 (**3**) and 1:2 (**4**) are possible (Figure 5). Thermodynamically, Gibbs free energies favor structure **3** by 9.2 kcal/mol. Thus, **3** has been selected as the reference point for the whole mechanism.

Metal Carbene Formation. Once the catalyst-alkene (**3**) complex is formed, it may undergo a direct dinitrogen extrusion in the presence of the alkene, which will be called as Mechanism 1. The other alternatives involve olefin nonassisted dinitrogen extrusion where the ethene will be lost from the catalyst-alkene complex prior to dinitrogen extrusion (Mechanism 2 and Mechanism 3).

Mechanism 1 (Scheme 1). In the olefin-assisted carbene transformation reaction the catalyst−alkene complex undergoes an N_2 extrusion step through transition state **5** (Figure 6), which requires 29.9 kcal/mol for activation. As the dinitrogen starts to detach from the molecule in **5**, the weakening of the N−C bond renders the carbon a highly reactive center to bind to copper. Copper is weakening its coordination to the alkene carbons, starting to make a strong bond with the central carbon atom in DMDM and undergoing pyramidalization as it proceeds to **6**. In **6**, a stabilizing interaction of 24.44 kcal/mol from the lone pair of copper to the antibonding orbital of alkene is found by the NBO analysis (LP Cu → BD* C═C 24.44 kcal/mol) (Figure 6). **6** further undergoes alkene loss through a transition-state structure (**7**) with a small free energy barrier of 2.0 kcal/mol (Scheme 1).

Alkene loss leads to the copper carbene complex structure **8** (Figure 7), whose details have been reported in our earlier study.[29] The length of the Cu−C bond is 1.771 Å, which is shorter than the experimental data for copper carbene

(28) Diaz-Requejo, M. M.; Nicasio, M. C.; Perez, P. J. *Organometallics* **1998**, *17*, 3051–3057.

(29) Çelik, M. A.; Yurtsever, M.; Tüzün, N. Ş.; Güngör, F. Ş.; Sezer, Ö.; Anaç, O. *Organometallics* **2007**, *26*, 2978–2985.

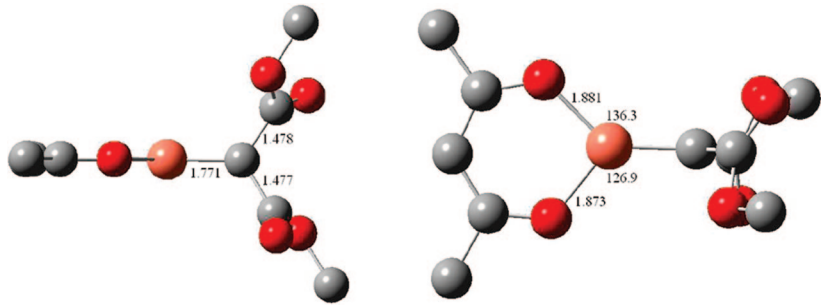

Figure 7. Three-dimensional geometrical structure of copper carbene complex **8** (top and side views).

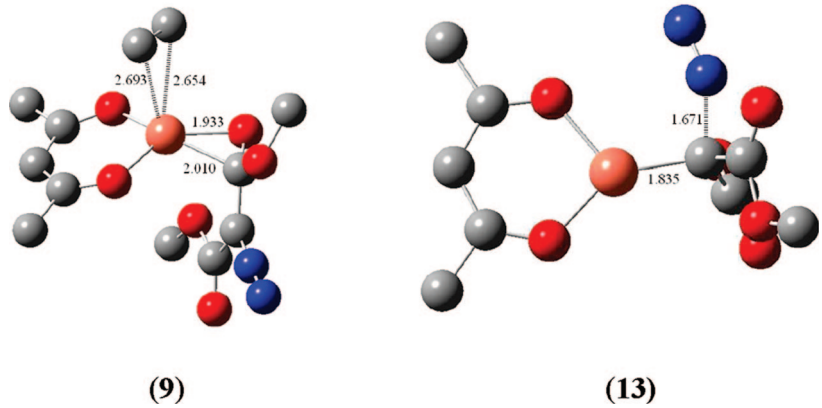

Figure 8. Three-dimensional geometrical structures of **9** and **13**.

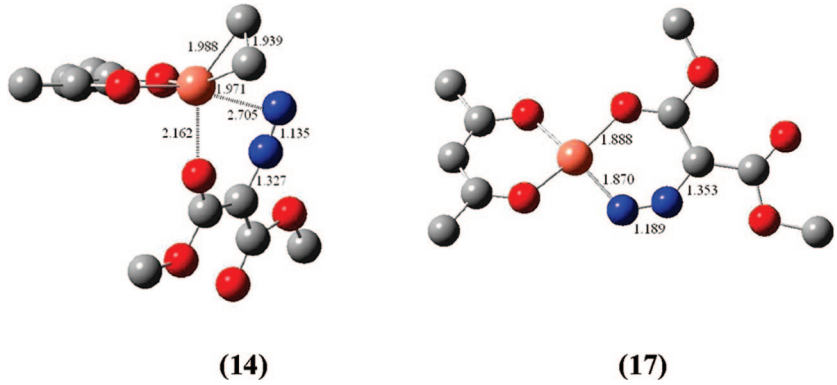

Figure 9. Three-dimensional geometrical structures of **14** and **17**.

complexes (1.834−1.888 Å).[30] This bond is 1.843 Å in **6**, which is shortened to 1.828 Å in the transition state **7** due to increased coordination to the carbene carbon. The plane of the ester groups is in an almost perpendicular position (the dihedral angle is 76.48°) with respect to copper carbene species because of the back-donation from one of the d orbitals of Cu to the empty p orbital of the carbene carbon. According to NBO analysis, the copper carbene contains a true copper−carbon double bond. As a result, the carbene carbon is sp^2 hybridized and the copper carbene complex has been reported to be a Fischer carbene.[29]

Mechanism 2 (Scheme 2). Alkene loss from the copper alkene complex prior to dinitrogen extrusion is tested in this mechanism. As copper attacks the electron-rich carbonyl double bond of DMDM, it detaches the alkene group (**9**) and yields the catalyst−DMDM complex **10** (Figure 8, Scheme 2). Cu then loses its coordination to the carbonyl bond and binds to the central DMDM carbon (structure **12**) by going through transition state **11**. In **12**, Cu is very close to the carbonyl group so that the copper center compensates for its coordination deficiency by making a favorable interaction with the carbonyl (Cu−C = 2.007 Å). Structure **12** has a Cu−C bond length of 1.939 Å, which becomes shorter during N_2 loss (1.835 Å in **13**) due to increased coordination between Cu and carbene carbon. The transition-state structure **13**, belonging to the N_2 extrusion step (Figure 8), has the highest Gibbs free energy value in the olefin-nonassisted mechanism. N_2 loss results in a copper carbene structure (**8**) that has already been discussed in mechanism 1.

Mechanism 3 (Scheme 3). This mechanism is initiated by the approach of the diazo compound to the catalyst−alkene complex to form a *κO,N* chelate complex through transition state **14** before alkene loss. In **14** (Figure 9), Cu starts to coordinate strongly to the carbonyl oxygen (2.162 Å) and N (2.030 Å) and weakens its coordination to the ligand and the alkene

(30) (a) Raubenheimer, H. G.; Cronje, S.; Olivier, P. J. *J. Chem. Soc., Dalton Trans.* **1995**, *2*, 313–316. (b) Dai, X.; Warren, T. H. *J. Am. Chem. Soc.* **2004**, *126*, 10085–10094.

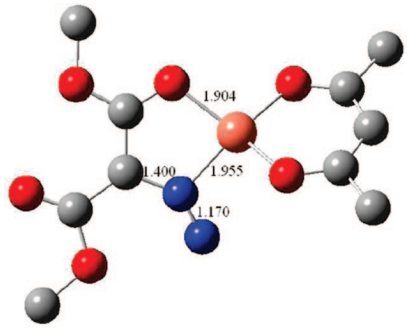

(22)

Figure 10. Three-dimensional geometrical structure of **22**.

substrate. This is reflected in $Cu-C_{alkene}$ (1.926 and 1.926 Å in **3** and 1.988 and 1.971 Å in **14**) and $Cu-O_{ligand}$ lengthenings (the $Cu-O_{ligand}$ bonds are 1.892 Å in **3** and 2.037 and 1.926 Å in **14**). Alkene loss takes place through transition state **16** with a small activation energy of 1.7 kcal/mol and gives the catalyst−diazo complex **17** as the product (Figure 9). According to kinetic studies on copper alkene complexes, an increase in the alkene concentration resulted in rate retardation.[28] This result has been interpreted by the existence of an equilibrium between catalyst−ethylene and catalyst−diazo complexes. The calculations on our system are in accordance with the kinetic studies, indicative of a pre-equilibrium before the N_2 extrusion.

An analogous structure of **17** has been determined by X-ray crystallography on an another Cu(I) catalyst with diazophenanthrone.[31] The Cu in **17** is almost square planar, as observed in X-ray data of the structure from the literature (the $O_{ligand}-Cu-O_{DMDM}-C_{DMDM}$ dihedral angle is 150.34°), and further attacks the uncoordinated nitrogen of the diazo (transition state **18**). Alternatively, copper can lose its diazo coordination and attack the π electrons of the C═O bond (**19**), giving **10** as the product in a single step. However, this transformation through **19** requires a barrier 11.5 kcal/mol higher than that of **18** with B3LYP/6-31G*, and this structure (**19**) could not be obtained as a transition state on the potential energy surface with BP86/SDD/6-31G* calculations. Thus, the stepwise process in mechanism 3 to form **10** is found to be more favorable.

Coordination to the terminal nitrogen in **20** is lost through transition state **21**, and structure **22** (Figure 10), which has two coplanar rings, is obtained. With the BP86/SDD/6-31G* methodology, IRC calculations on **18** gave **22** directly. The calculations on this system have shown that the nonbonded interactions in the modeled structures are stronger in general with B3LYP/6-31G* as compared to BP86/SDD/6-31G*; thus with the B3LYP/6-31G* methodology, copper cannot lose its coordination in a single step and reaching **22** in a stepwise manner is a more facile process. The NMR chemical shifts of a structure analogous to **20** have been reported in a study on a stable platinum α-carbonyl diazoalkane complex, and it has been stated that this platinum complex might be regarded as a model for copper(I) complexes.[32]

Copper leaves the nitrogen and forms **10** by its coordination to the π electrons of the carbonyl group. Structure **10** further undergoes olefin-nonassisted N_2 extrusion step as in mechanism 2.

(31) Straub, B. F.; Rominger, F.; Hofmann, P. *Organometallics* **2000**, *19* (21), 4305–4309.
(32) (a) Straub, B. F.; Rominger, F.; Hofmann, P. *Inorg. Chem. Commun.* **2000**, *3*, 214–217. (b) Straub, B. F.; Hofmann, P. *Inorg. Chem. Commun.* **1998**, *1*, 350–353.

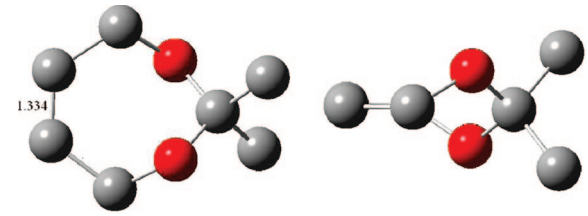

Figure 11. Three-dimensional geometrical structure of the dioxepine (top and side views).

In the transformation of the copper ethene complex **3** to the copper DMDM complex, copper can attack at the central carbon of DMDM or at only nitrogen or oxygen rather than attacking both of them at the same time. The attack at the central carbon enforces N_2 extrusion (**5**), as shown in mechanism 1. The *κO*- or *κN*-coordinated intermediates could not be obtained by B3LYP/6-31G* or BP86/SDD/6-31G* calculations.

Among the carbene formation pathways, mechanism 3 should be a more facile route for this system. Although the overall reaction barrier is only slightly lower in mechanism 3 as compared to mechanism 1, this difference may render mechanism 3 almost 14 times faster than mechanism 1 at the reaction temperature (80 °C). The BP86/SDD/6-31G* calculations predict a difference in energies between the rate-determining steps of the mechanisms even greater than that of the B3LYP/6-31G* results. The experimental prequilibrium[14] before the rate-determining N_2 loss is also observed in mechanism 3. More importantly, the experimental evidence for the existence of structures analogous to **17** and **20** also support the preference for mechanism 3.[31,32] Thus, these points that we put forward above may render mechanism 3 a more favorable pathway as compared to the others for this system. For other systems, where such an assistance from the carbonyl group is not present, mechanism 1 can serve as a facile alternative.

Real System. To verify the suggested mechanisms, the test molecule 2,2-dimethyl-4,7-dihydro-1,3-dioxepine (Figure 11), which has been reported to undergo successful cyclopropanation in the presence of DMDM and $Cu(acac)_2$, has been used.[17] In the carbene formation, structure **13**, bearing a dioxepine substrate, has the lowest energy on the reaction diagram (31.7 kcal/mol for **5** in mechanism 1 and 28.4 kcal/mol for **13** in mechanisms 2 and 3, respectively). Considering the experimental evidence in the model compound and the energetics observed with the dioxepine substrate, mechanism 3 can be suggested as a more probable pathway for this system (Scheme 3). As in the model case, mechanism 1, which does not require any assistance from the carbonyl group, may be a facile reaction path for diazo compounds without carbonyl group(s).

The BP86/SDD/6-31G* calculations on mechanisms 1−3 differ from the B3LYP/6-31G* calculations mainly in the first barriers, and the energies of almost all stuctures relative to starting compounds (structure **3**) are systematically higher with the BP86/SDD methodology, although most of the barriers on the paths are almost unchanged. To understand the effect of changing the basis set and the functional separately, calculations have been performed with the BP86/6-31G* and B3LYP/SDD/6-31G* methodologies on some structures. Bond lengths of **3**, calculated by four methodologies, are dependent on the basis set rather than the functional (Figures S2−S4 in the Supporting Information). Likewise, the barriers of the transition **3** → **5** in mechanism 1 at the B3LYP/SDD/6-31G* and BP86/6-31G* levels are 43.4 and 24.5 kcal/mol, respectively, pointing out the effect of the basis set rather than the functional on copper. In the B3LYP/6-31G* calculations, the copper center interacts

Scheme 4. Cyclopropanation through a Three-Centered Transition State[a]

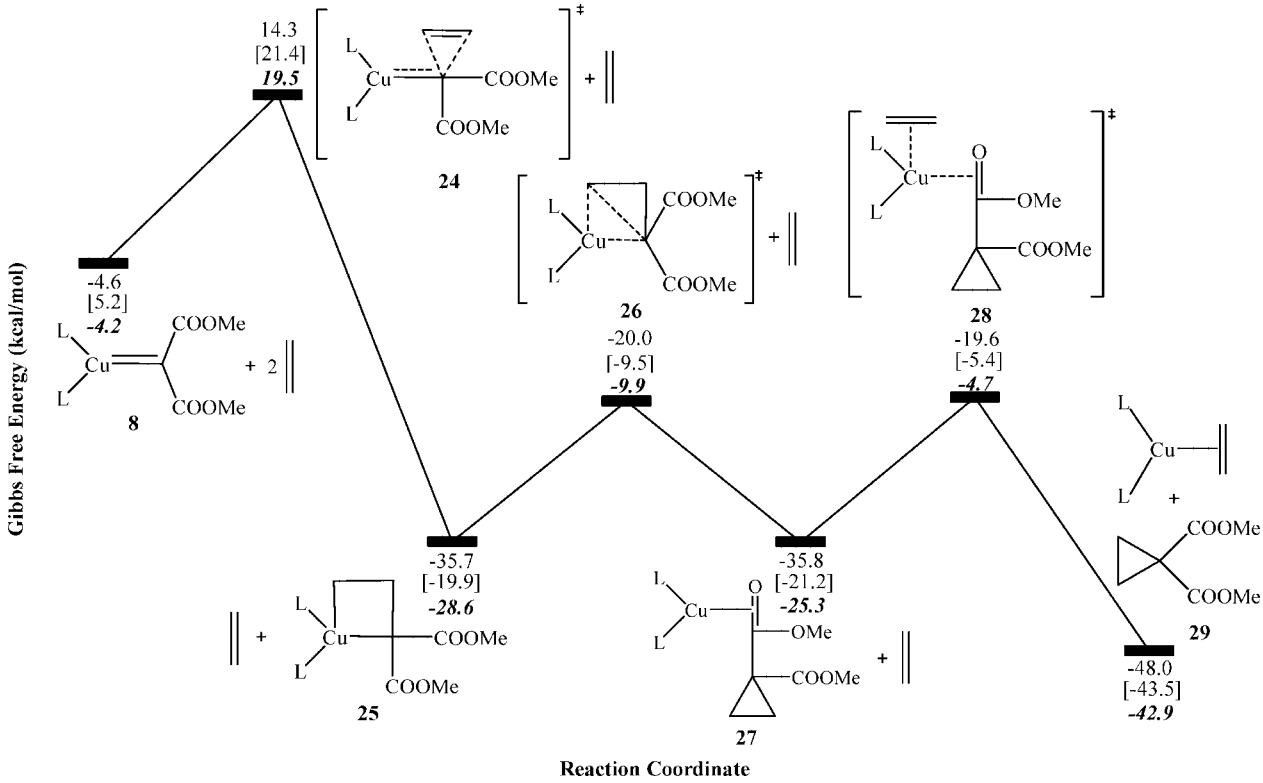

[a] Gibbs free energies are relative to **3** and DMDM. Values in parentheses refer to BP86/SDD/6-31G* results with ethene, and bold italic values refer to B3LYP/6-31G* calculations with dioxepine as substrate.

strongly with the lone pairs and electron-rich centers, whereas BP86/SDD/6-31G* calculations do not reproduce the strong long-range or bonding interactions. These effects are carried along all the way on the path, since copper is the main reaction center; thus, barriers other than the first ones are almost unchanged. The differences in the two methodologies are reflected in longer nonbonding and bonding distances of copper with the BP86/SDD/6-31G* methodology as compared to those with B3LYP/6-31G*.

Cyclopropanation Stage

Three-Centered Pathway (Scheme 4). The three-centered pathway of cyclopropanation starts by the attack of the carbene carbon at the alkene through a three-centered transition-state structure (**24**) (Figure 12). As the ethene molecule approaches the copper carbene system in **24**, the metal weakens its coordination to carbene C (Cu−$C_{carbene}$ = 1.811 Å) and starts to interact with the alkene carbons at distances of 2.531 and 2.190 Å. IRC calculations on **24** revealed a metallacyclobutane intermediate (**25**) (Figure 12). Transition state **26** gives a cyclopropane product (**27**), in which the copper center interacts with π electrons of the carbonyl bond, providing coordinative saturation of the Cu center. Assistance of a second alkene is needed in order to free the catalyst and the cylopropane product. Forming a naked catalyst directly from **27**, without alkene assistance, causes this step to become highly endergonic (44.03 kcal/mol). The second alkene interacts with the copper center, which further weakens its coordination to the C=O double bond (transition structure **28**) and finally the catalyst−alkene complex detaches from the system and cyclopropane (**29**) is obtained.

Four-Centered Pathway. Attack of the copper carbene complex at olefinic carbons via a four-centered transition

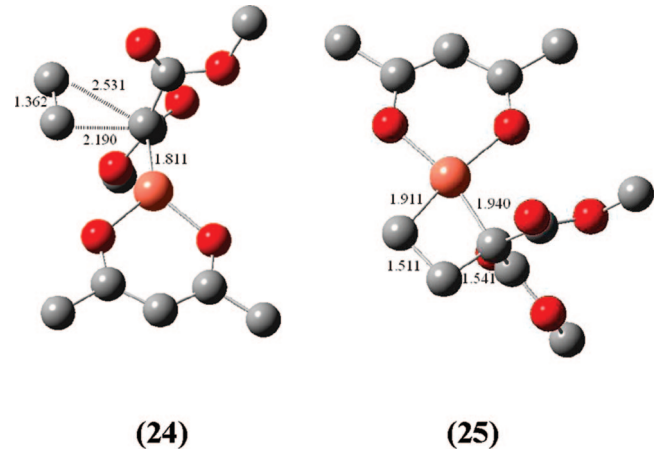

Figure 12. Three-dimensional geometrical structures of **24** and **25**.

structure is expected to form a metallacyclobutane intermediate. However; in our calculations, reaction of ethene with the copper carbene complex **8** to form a metallacyclobutane revealed structure **6** (Scheme 1) as the reactant from its IRC calculations, contrary to expectations. **6** will resist further cyclopropanation through a four-membered transition state to form metallacyclobutane, since this transition state required a barrier of 5.6 kcal/mol (Figure S5, Supporting Information), whereas its alkene loss as in mechanism 1 is almost barrierless. Moreover, this process does not lead to a metal carbene, although the existence of copper carbene formation has been proved.[10] Thus, this alternative step is eliminated.

Another path to metallacyclobutane formation is via rotation of the diester moiety **30** to give the isomer **31** (Scheme 5) of **8**

Scheme 5. Cyclopropanation through a Four-Centered Transition State[a]

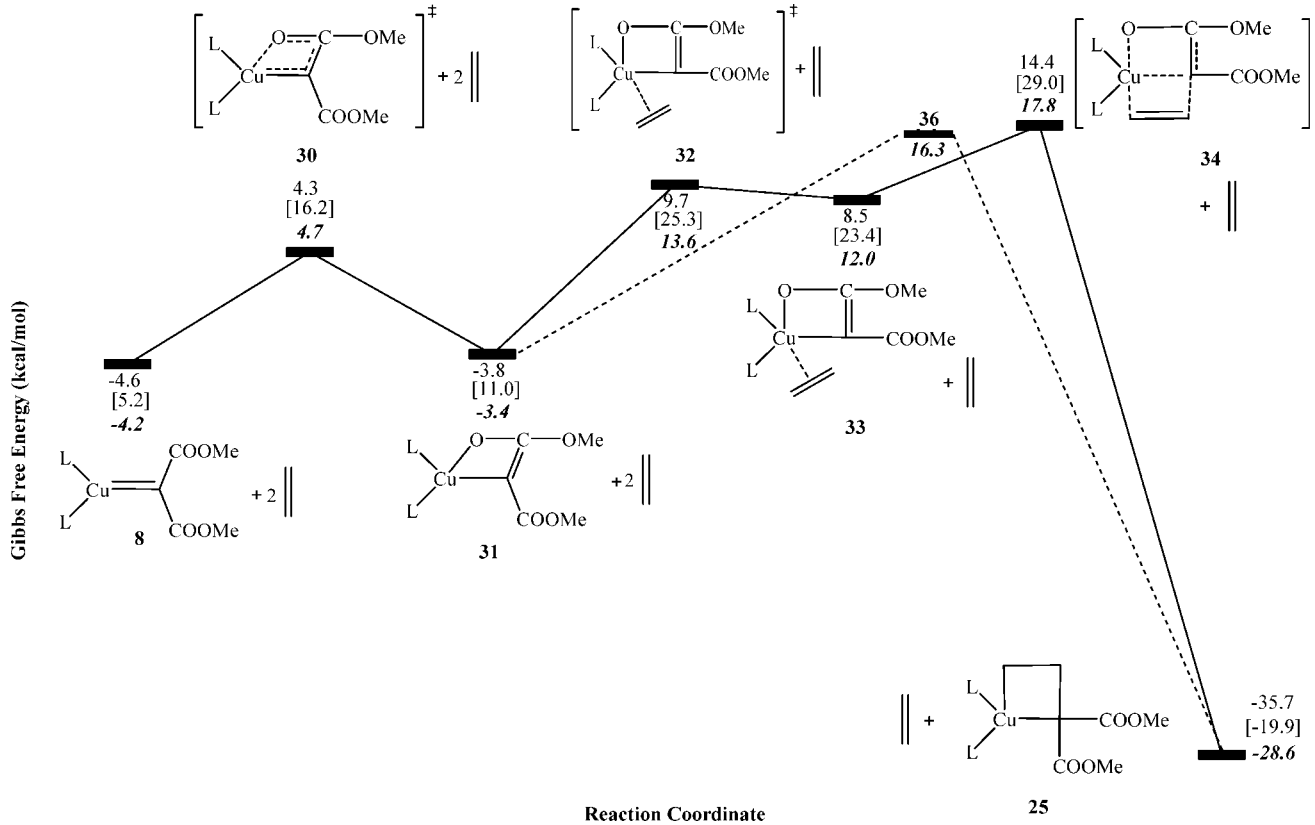

[a] Gibbs free energies are relative to **3** and DMDM. Values in parentheses refer to BP86/SDD/6-31G* results with ethene, and bold italic values refer to B3LYP/6-31G* calculations with dioxepine as substrate.

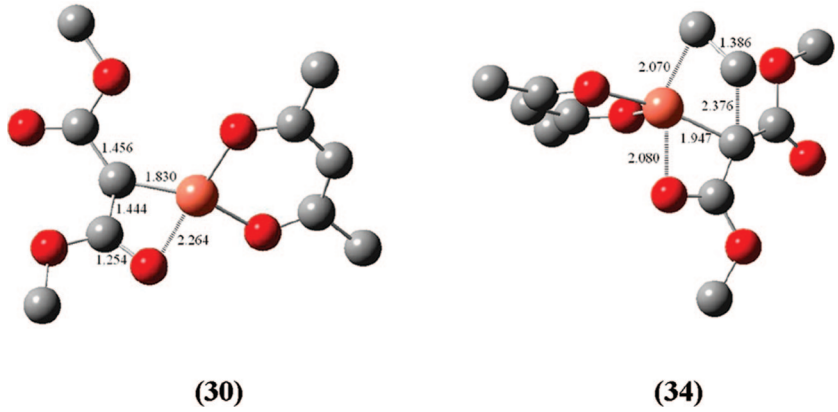

Figure 13. Three-dimensional geometrical structures of **30** and **34**.

with a favorable Cu—O interaction (Cu—O distance of 2.264 Å) (Figure 13). In this geometry, the carbene carbon is sterically more susceptible to interact with the p orbitals of the ethene, as seen in transition state **32**. In **8**, this interaction was hindered by the perpendicular orientation of the bulky ester groups with respect to the catalyst plane. Before the four-centered transition state (**34**), an intermediate is formed (**33**) where the copper center interacts with the π electrons of the alkene, at the expense of making weaker bonds with its ligand and its substrate, increasing its energy. Metallacyclobutane formation from **33** will be a facile reaction, since only a shift of one of the alkene carbons is required to make an efficient overlap (transition state **34**, Figure 13). The rest of the path is exactly the same as in the three-centered pathway.

Another alternative way of cyclopropanation can be through double alkene complexation to the active catalyst. This mechanism starts with structure **3**, and then structure **6** forms through **5**, as in mechanism 1. At this point, a second alkene molecule can approach the carbene carbon via transition state structure **35**, shown in Figure 14. Energetically, 17.6 kcal/mol of Gibbs free energy is required for activation of this transition-state structure. This amount of Gibbs free energy makes the mechanism unfavorable, because 2.0 kcal/mol of Gibbs free energy is sufficient for alkene extrusion that will lead it to a copper carbene complex (Scheme 1). Thus, it can be concluded that cyclopropanation does not take place through this mechanism.

In the studied pathways, the highest points reached in three- and four-centered mechanisms are energetically the same with

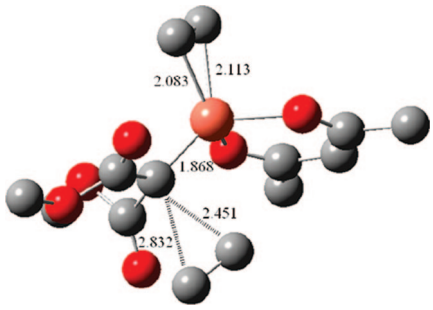

Figure 14. Three-dimensional geometrical structure of complexation of double alkene **35**.

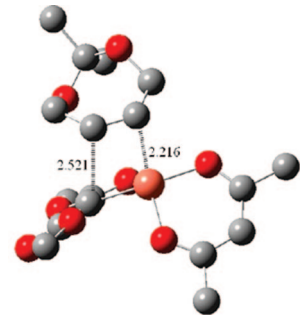

Figure 15. Three-dimensional geometrical structure of **36**.

the B3LYP/6-31G* calculations (Schemes 4 and 5), inhibiting an effective selection between the paths in the model case. Both mechanisms involve facile steps which are accessible at the reaction temperature. Metallacyclobutane is the common intermediate in both of the pathways. In cyclopropanation, when the carbene approaches the alkene in **24**, the carbene carbon starts to adopt a sp^3 geometry and the bulky ester groups have to rotate away from the reaction centers to enable a suitable site for the attack. However, in the four-centered pathway, the planar geometry of **31** facilitates an effective attack and overcomes a smaller barrier at this step as compared to that of **24**. Geometry optimizations of **24** and **34** in benzene, using IEF-PCM methodology at the B3LYP/6-31G* level, have not made a significant difference ($\Delta\Delta G^{\ddagger} = 0.63$ kcal/mol). On the other hand, BP86/SDD/6-31G* results showed a clear distinction between the two paths (Schemes 4 and 5); however, this difference may stem from the Cu−O interactions, which are stabilized more in the B3LYP/6-31G* calculations and which are essentially important in the four-centered pathway.

Real System. The steric effect of the dioxepine substrate increased the barriers of three- and four-centered mechanisms by at most 5 kcal/mol as compared to the model compound. Although a concerted transition structure from **31** to **25** could not be located with the model compound, a transition state could be found with dioxepine substrate at a relative energy of 16.3 kcal/mol. Thus, this new point (**36**) (Figure 15) is considered instead of **34**. With a dioxepine substrate, the B3LYP/6-31G* level of calculations favor a four-centered pathway over a three-centered pathway (**36** vs **24**) by 3.2 kcal/mol, whereas BP86/SDD/6-31G* calculations prefer **24** over **36** (by 8.1 kcal/mol) as in the model study. No experimental data favor either of these two mechanisms for this system. From the B3LYP calculations in this study, it can be expected that when the diazo compound bears carbonyl group(s), a four-centered pathway via carbonyl assistance can be an alternative to the three-centered pathway. The calculations with dioxepine substrate have revealed that the chair type of product, reported to be produced from the experimental study,[17] was unfavorable by 3.60 kcal/mol compared to the boat conformer. The calculations on the dioxepine substrate have also shown that the boat conformer of the ring is preferred by 3.26 kcal/mol over the chair. High basis set calculations (B3LYP/6311+G**) or high-temperature results (T = 80 °C) did not change the trend. Furthermore, the preference for the boat conformer of dioxepine has also been supported by the NMR results of St. Jacques and co-workers.[33] The cyclopropanation reaction is completed with a cyclopropane product, which is dimethyl 4,4-dimethyl-3,5-dioxabicyclo[5.1.0]-octane-8,8-dicarboxylate.

(33) Blanchette, A.; Sauriol-Lord, F.; Jacques, St. *J. Am. Chem. Soc.* **1978**, *100*, 4055–4062.

Conclusion

The mechanism of the copper(I)-catalyzed olefin cyclopropanation reaction with dimethyl diazomalonate (DMDM) has been extensively investigated using DFT methods at the B3LYP/6-31G* and BP86/SDD/6-31G* levels in this study. In the first part, three possible pathways for copper carbene formation have been studied. In the transformation of copper ethene (**3**) to a copper DMDM complex, copper can attack the central carbon of DMDM (mechanism 1) or the carbonyl group of DMDM (mechanism 2), or only nitrogen, only oxygen, or nitrogen and oxygen at the same time (mechanism 3). κO- or κN-coordinated intermediates could not be obtained by B3LYP/6-31G* or BP86/SDD/6-31G* calculations and the $\kappa O,N$ coordination in mechanism 3 required the lowest barrier. From the calculations, alkene-nonassisted diazo extrusion via a $\kappa O,N$ complex (**17**) is suggested as a favorable route over direct nitrogen gas extrusion in the presence of the alkene. The former mechanism involves assistance from the C═O group of DMDM, and the experimental evidence for the existence of intermediates in the literature analogous to structures **17** and **20** involved in this pathway supports the preference for this mechanism. Additionally, N_2 gas extrusion is the rate-determining step, as expected from the experiments and calculations in the literature. In cases where such a favorable C═O interaction is not favored or the diazo compound does not bear carbonyl group(s), direct nitrogen gas extrusion in the presence of alkene (mechanism 1) can be a facile alternative. With dioxepine as the substrate, the difference between the overall barriers of mechanisms 1 and 3 becomes more pronounced, supporting the preference of mechanism 3 for this system.

In the cyclopropanation part, two mechanisms were suggested: direct addition to carbene carbon via a three-centered pathway and cyclopropanation via a four-centered activated complex, giving a metallacyclobutane intermediate. With the model compound, three- and four-centered pathways involved facile steps accessible at the reaction temperature and the overall barriers were almost the same. In both mechanisms, metallacyclobutane is the common intermediate and the four-centered pathway required assistance from the C═O group. With dioxepine as the substrate, when the diazo compound has carbonyl group(s), the four-centered path, involving favorable interactions between copper and the carbonyl group, appears to be a more facile route, whereas the three-centered pathway via direct alkene addition is also a probable facile route for diazo compounds without a C═O group. The BP86/SDD calculations favored the three-centered pathway with both model substrate and the dioxepine, in contrast to the findings of B3LYP/6-31G* calculations. It has been observed that the nonbonding interactions between the copper center and the carbonyl or azo group are treated more strongly in the B3LYP/6-31G* method than in BP86/SDD/6-31G*. Thus, the methodology is important in

the accurate prediction of energies and geometries and should be aided by the experimental data.

Acknowledgment. We gratefully acknowledge the ITU Informatics Institute High Performance Computing Center and UYBHM (Grant No. 20202007) for the computer time provided, the TUBITAK for Grant Nos. 104T403 and 105E067, and the ITU Research Fund (Grant No. 30631). We also thank Naciye Talınlı, Olcay Anaç, Özkan Sezer, Aylin Konular, and Mine Yurtsever for fruitful discussions.

Supporting Information Available: Tables and figures giving Cartesian coordinates of all reported structures, numbers of imaginary frequencies, total electronic and zero-point vibrational energies, and Gibbs free energies of all the structures discussed in the paper. This material is available free of charge via the Internet at http://pubs.acs.org.

OM800094K